

Irreversibility and rate dependence in sheared adhesive suspensions

Zhouyang Ge^{1,2,*}, Raffaella Martone³, Luca Brandt¹, and Mario Minale^{3†}

¹ Department of Engineering Mechanics, KTH Royal Institute of Technology, SE-100 44 Stockholm, Sweden

² Department of Mechanical Engineering, University of British Columbia, Vancouver, BC, V6T 1Z4, Canada and

³ Department of Engineering, University of Campania “Luigi Vanvitelli”,

Real Casa dell’Annunziata, via Roma 29-81031 Aversa, CE, Italy

(Dated: June 29, 2021)

Recent experiments report that slowly-sheared noncolloidal particle suspensions can exhibit unexpected rate(ω)-dependent complex viscosities in oscillatory shear, despite a constant relative viscosity in steady shear. Using a minimal hydrodynamic model, we show that a weak interparticle attraction reproduces this behavior. At volume fractions $\phi = 20 \sim 50\%$, the complex viscosities in both experiments and simulations display power-law reductions in shear, with a ϕ -dependent exponent maximum at $\phi = 40\%$, resulting from the interplay between hydrodynamic, collision and adhesive interactions. Furthermore, this rate dependence is accompanied by diverging particle diffusivities and pronounced cluster formations even at small oscillation amplitudes γ_0 . Previous studies established that suspensions transition from reversible absorbing states to irreversible diffusing states when γ_0 exceeds a ϕ -dependent critical value $\gamma_{0,\phi}^c$. Here, we show that a second transition to irreversibility occurs below an ω -dependent critical amplitude, $\gamma_{0,\omega}^c \leq \gamma_{0,\phi}^c$, in the presence of weak attractions.

The flow properties of suspensions remain challenging to predict despite the tremendous progress to date. Even the simplest suspensions, consisting of non-Brownian particles suspended in a density-matching Newtonian fluid, while exhibiting a Newtonian behavior in steady shear (SS) flow, can show very rich phenomena under oscillatory shear (OS), such as flow irreversibility and chaos [1], absorbing state transitions [2, 3], and microstructure reorganizations at large accumulated strains [4, 5]. All these fundamental behaviors are predicted using very few ingredients in the equations of motion that are in order: hydrodynamic forces, including lubrication between adjacent particles, and hard-sphere collisions. Because the latter do not possess any characteristic time scale and their amplitude is proportional to the driving hydrodynamic force, the system and all its material functions are rate-independent [6, 7].

So far, it has been assumed that the suspension microstructure depends on the strain amplitude (γ_0) and strain history (γ_{tot}) in OS, and rate dependence (if any) is manifested in both SS and OS. However, recent experiments challenge this assumption and demonstrate a frequency (ω)-dependent rheology in OS in the absence of any rate-dependence in SS [8–10]. These authors demonstrate that, in OS, the suspension viscosity only depends on the maximum shear rate ($\gamma_0\omega$) and that data taken at different volume fractions (ϕ) can be rescaled on a single master curve, so to highlight a universal behavior of these materials. Furthermore, this rheological observation questions the physics of self-organization in the simplest driven noncolloidal suspension: it was assumed that suspensions undergo transitions from reversible absorbing states to irreversible chaotic states if γ_0 exceeds a ϕ -dependent critical amplitude, $\gamma_0^c(\phi)$, independent of the driving frequency [1, 2, 11]; now the experiments in [10] may imply that ω also affects irreversibility.

In this Letter, we combine experiments with simulations and show that a weak interparticle attraction (e.g. van der Waals force) is enough to induce the sought rate dependence in OS, while keeping the SS behavior rate-independent. Moreover, we reveal that this rheological behavior in OS is accompanied by enhanced particle diffusivities and cluster formations below a critical shear rate, thus the onset of rate dependence when reducing γ_0 is closely related to the threshold for irreversibility. A deeper understanding of self-organization and dynamical phase transition in suspensions is not only of fundamental interest [12–15], but has also attracted practical attention due to its applications in hyperuniform photonic materials or suspension flow control [16–18]. This letter shows that a physical ingredient up to now neglected, *i.e.* interparticle attraction, must be taken into account.

Our experimental samples consist of glass hollow microspheres (5~50 μm in diameter, mean 15.4 μm) dispersed in a Newtonian fluid (polyisobutene, viscosity 15.8 Pa·s at 21.2°C) at three volume fractions (20~40%). Time sweep oscillatory tests are executed on a constant-strain rheometer, ARES G2 (TA Instruments) equipped with a cone-and-plate geometry, by imposing a sinusoidal strain during each run, $\gamma(t) = \gamma_0 \sin(\omega t)$, for γ_0 from 0.5% to 2 and ω from 5 to 200 rad/s. After a steady preconditioning shear, the complex viscosity is followed in time in units of the total accumulated strain, $\gamma_{tot} = 4\gamma_0 n_{cyc}$, where n_{cyc} is the number of cycles of the oscillatory shear. All tests are performed repeatedly according to standard protocols, cf. Ref. [10].

The suspensions are inertialess and non-Brownian, as the particle Reynolds number is smaller than 10^{-6} and the Péclet number is larger than 10^5 . Particle sedimentation can be neglected, as the average Shields number is about 10^3 . A characteristic time arising from Brownian diffusion or sedimentation is thus irrelevant in the inves-

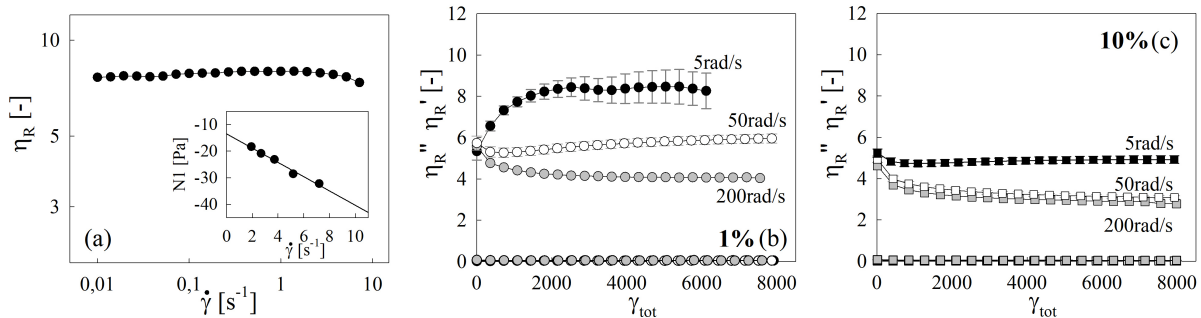


FIG. 1: Experiment at $\phi = 40\%$: (a) Relative viscosity (η_R) and first normal stress difference (N_1 , inset) vs. shear rate in SS. (b,c) Evolution of the dynamic viscosity (η'_R) and its elastic counterpart (η''_R) vs. the total accumulated strain at $\gamma_0 = 1\%$ (b) and 10% (c) in OS. The angular frequencies are indicated in the figure.

tigated suspensions and, accordingly, the SS behaviour shows constant viscosity and first normal stress difference negative and linear in the shear rate; see Fig. 1(a). In OS, the relative complex viscosity, $\eta_R^* \equiv \eta'_R - i\eta''_R$, evolves in time and is a function of γ_0 , as widely reported in the literature [2, 4, 19]; but, surprisingly, it also decreases with ω (*i.e.* shear thinning). To illustrate this, we display in Fig. 1(b,c) the relative dynamic (η'_R) and elastic (η''_R) viscosities vs. γ_{tot} , for two values of γ_0 and three of ω at $\phi = 40\%$ (data for other ϕ are available in Ref. [10]). η'_R is always about two orders-of-magnitude larger than η''_R , thus it is practically coincident with η_R^* , highlighting the viscous behavior of the suspension. In general, an ω -dependent regime is observed for $\gamma_0 \lesssim 1$ and an ω -independent regime otherwise. These two regimes coincide with those observed by Lin et al. [20], who showed that in the first regime the microstructure self-arrangement is driven by shear-induced particle diffusions, while in the second one the microstructure is immediately formed by the oscillation itself, similarly to what happens for a steady flow reversal that is indeed rate-independent. The dependence on the frequency and the importance of diffusion indicate that a *non-hydrodynamic* force is at play [21], which cannot be hard-sphere interactions. To identify this force, we now turn to numerical simulations.

Discrete element simulations based on a minimal hydrodynamic model are performed for suspensions at zero Reynolds number [22]. Specifically, our model determines particle nonaffine trajectories according to lubrication, contact (hard-sphere) and interparticle potentials, similarly to the Stokesian dynamics [23]. Since the full many-body hydrodynamic interactions are truncated at the level of lubrication, our method is mostly accurate for dense suspensions where interparticle gaps are small, cf. Refs. [24, 25]. The results below are therefore for $\phi = 40\%$ and 50% [26].

To begin with, we note that several forces have been

linked in the literature to rate dependence (shear thinning in particular) in dense, non-Brownian suspensions: (normal-)load-dependent friction [27], electrostatic repulsion [24, 28] and van der Waals attraction [29, 30]. Friction, as well as any other possible dissipation mechanisms due to surface roughness, should lead to no less rheological response in SS than OS, since larger deformations activate more frictional contacts at the same ϕ . Indeed, we have checked that including the contact model of [27] in our system gives shear-thinning in SS instead of OS, contrary to what the experiments show. Therefore, an explanation in terms of friction is unlikely.

As for electrostatic repulsion, its impact on the suspension rheology can be understood as an effective volume effect [28]. At low shear (thus stress), few particle pairs come closer than an enlarged radius due to the finite-range repulsive force; the portion of such particles (thus the effective ϕ) reduces with the shear, leading to shear thinning. Although plausible, it is difficult to rigorously establish this argument in all scenarios. In fact, our simulations show that electrostatic repulsion causes shear thickening in OS, again contradicting the experimental results [31].

The only possibility left is attraction. Here, we consider the simplest van der Waals (vdW) attraction, which is always present regardless of particle size [32, 33]. As in Ref. [30], we model a nonretarded and additive vdW as $F_{vdw} = A\bar{a}/12(h^2 + \epsilon^2)$, where A is the Hamaker constant, $\bar{a} = 2a_i a_j / (a_i + a_j)$ the harmonic mean radius of two interacting particles, h their surface gap and ϵ a small constant to prevent divergence of F_{vdw} at $h = 0$; we use $\epsilon = \sqrt{10^{-5}}a$ to model glass beads. The maximal attraction $\mathcal{F} = Aa/12\epsilon^2$ introduces a characteristic stress scale, $\tau_{\mathcal{F}} = \mathcal{F}/\pi a^2$, for two touching particles, opposed to the minimal shear stress, $\tau_s = \eta_0 \gamma_0 \omega / 2\pi$ ($\eta_0 \dot{\gamma}$ in SS), where η_0 denotes the solvent viscosity. The ratio $\tau_s / \tau_{\mathcal{F}}$ thus defines a non-dimensional shear rate, hereafter denoted $Sr \equiv 6\eta_0 \epsilon^2 a \gamma_0 \omega / A$.

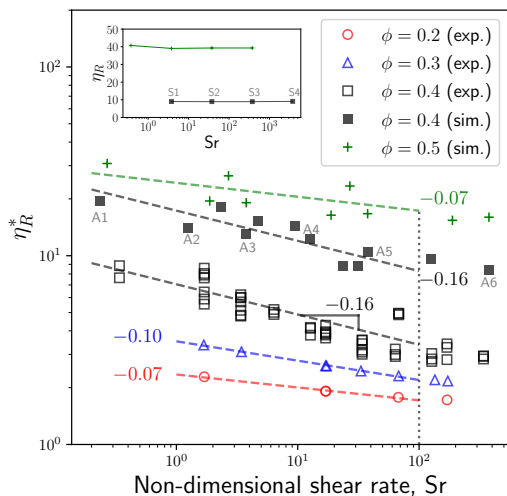


FIG. 2: Suspension viscosities in OS and SS (inset). Dashed lines are least squares fits to data for $Sr < 100$; numbers indicate the slopes.

Fig. 2 shows the rheology of this model adhesive system. Remarkably, with the addition of only a weak vdW attraction ($\propto 1/Sr$), the essential features of the complex rate-(in)dependent behaviors in (SS)OS seen in experiments are captured numerically [34]. Specifically, below a critical shear rate in OS, η_R^* exhibits power-law reductions with shear, $\eta_R^* \sim Sr^{-\alpha}$, with α a ϕ -dependent positive exponent largest at $\phi = 40\%$. This non-monotonic dependence can be understood by considering the limits of very dilute and highly-packed suspensions: at vanishing volume fractions, collisions and vdW attractions are negligible, the system is dominated by hydrodynamic forces and therefore nearly rate-independent; close to packing, lubrication and contact forces dominate but, because both are proportional to the shear rate, the system again exhibits weak rate dependence.

To provide quantitative evidence, we display the different contributions to the relative viscosity for ten representative cases in Fig. 3. The budget terms correspond to the Stokes (stk), lubrication (lub), contact (ctt) and vdW forces extracted from the simulations [22]. Surprisingly, at $\phi = 40\%$, where the maximum vdW effect is expected, virtually no contributions from the attractive vdW forces are visible across three decades of Sr . In SS, the lubrication and contact stresses are constant (stk only depends on ϕ thus identical in all cases) and so the relative viscosity; in OS, however, lubrication is shear-dependent while contact stresses are vanishing. Since the rate dependence results from vdW, naively, one would expect it also makes a rate-dependent contribution to the stress budget, or at least be active in OS. Its absence implies that the rheology is *indirectly* modulated by weak attractions. The question, then, is how such indirect modulation occurs.

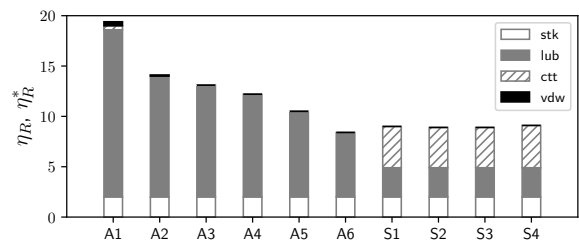


FIG. 3: Shear stress components of representative OS and SS cases at $\phi = 40\%$; see Fig. 2 for the annotation.

Recall that, without any inertial, thermal or non-Newtonian effects, the rheological properties of a suspension at any given time are determined solely from its underlying microstructure [33]. The microstructure evolution is mediated by time-reversible Stokes flows, though the particle dynamics themselves satisfy Onsager's variational principle for general irreversible processes [35]. Indeed, both experiments and simulations have shown that particle diffusion can occur in slowly sheared suspensions, leading to irreversible and ultimately chaotic dynamics [1, 21, 36–38]. Particularly, in OS, the threshold for irreversibility was found to be gauged by a ϕ -dependent critical strain amplitude $\gamma_0^c(\phi)$: for $\gamma_0 > \gamma_0^c$, suspensions are irreversible with non-vanishing effective diffusivities, $D_i = \langle (\Delta_i/a)^2 \rangle / 2\gamma_{tot}$ (Δ_i denotes the particle displacement in any spatial direction i at integer-period intervals); for $\gamma_0 < \gamma_0^c$, the dynamics evolve towards absorbing states with $D_i \approx 0$ in finite time. The system undergoes a continuous phase transition (likely conserved directed percolation [15]) at $\gamma_0 = \gamma_0^c$, indicated by a nonzero order parameter $\langle f_a^\infty \rangle$ based on the mean fraction of actively colliding particles. This theoretical framework [2] applies to a remarkable variety of situations, see e.g. Ref. [15] and references therein. We note that none of them invokes a role for frequency, though.

It is therefore natural to examine the microstructure statistics of our suspensions. Fig. 4 shows the numerical results at $\phi = 40\%$ and 50% . Surprisingly, at strain amplitudes well under the irreversibility threshold just mentioned ($\gamma_0 \leq 0.2$ for all simulations with $\gamma_0^c \approx 0.82$ at $\phi = 40\%$ [39]), our suspensions can be both irreversible and active. This irreversibility only occurs below a fixed critical shear rate, Sr_c . Fig. 4(a) shows that, by renormalizing the effective diffusivities with their averages in the infinite shear limit, e.g. $D_x^\infty = \langle D_x \rangle|_{Sr \rightarrow \infty}$, all values at $\phi = 40\%$ and 50% diverge with reducing Sr . A similar behavior is observed for the order parameter, which diverges below Sr_c as $\langle f_a^\infty \rangle \sim Sr^\beta$, with $\beta = -0.40$ (Fig. 4b). Akin to the self-organized criticality due to slow sedimentation [3], particles in adhesive suspensions actively form clusters with a near power-law size distribution (Fig. 4c). As an example, Fig. 4(d) shows a snap-

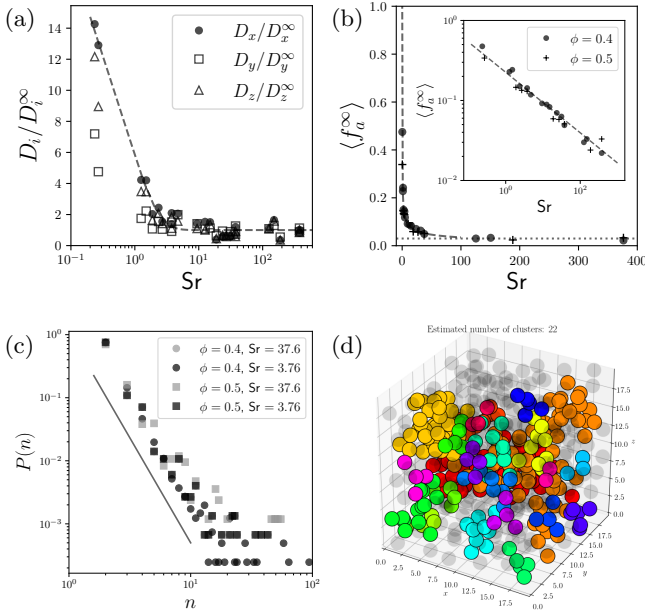


FIG. 4: Microstructure statistics in OS. (a) Relative particle diffusivities at $\phi = 40\%$ and 50% (not distinguished). The dashed line is a fit of D_x/D_x^∞ . (b) Mean fraction of active (colliding) particles on linear and logarithmic (inset) scales. The dashed line is a power-law fit with slope $\beta = -0.40$. (c) Power-law distribution of cluster size, $P(n) \sim n^{-3.33}$ (solid line). (d) A snapshot of the particle suspension at $\phi = 40\%$. Different cluster groups are indicated by colors.

shot of the suspension at $\phi = 40\%$, where various particle clusters are displayed in color (inactive particles are displayed in grey).

Comparison of Figs. 4(a,b) and 2 indicates that this new threshold for irreversibility is closely related to the onset of rate dependence, both at $Sr_c \approx 100$ [40]. Below Sr_c , the microstructure is indirectly modulated by weak vdW interactions; their relative intensity is inversely proportional to the shear rate, thus the suspension shows diffusive dynamics and rate dependence at low γ_0 . Above Sr_c , hydrodynamic interactions overcome vdW, resulting in time-reversible Stokesian dynamics and a rate-independent suspension rheology. Here, we cannot determine the value of Sr_c exactly due to the increasing uncertainties in the data near it. Nevertheless, by matching experiments and simulations at $Sr_c = 100$ (Fig. 2), we estimate the Hamaker constant of the vdW interaction to be $A \approx 4 \times 10^{-19}$ J in the system under investigation. This is within the range of A for most condensed phases (cf. Ref. [32], page 254), which validates our assumption.

More importantly, the existence of a unique Sr_c suggests that there is a *frequency-dependent* critical amplitude for the transitions between absorbing and diffusing

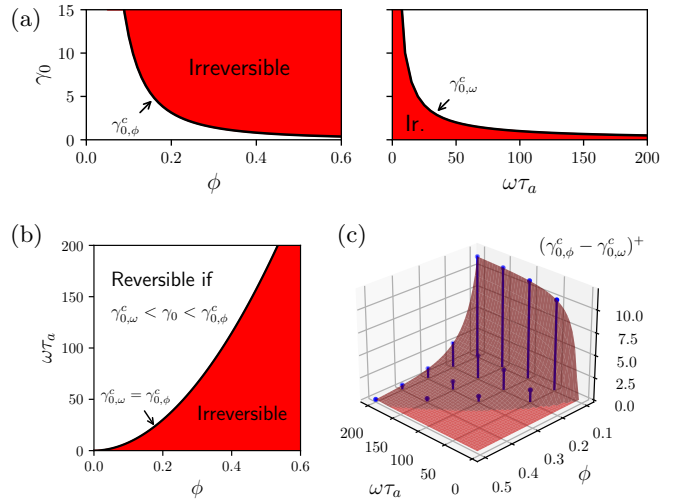


FIG. 5: Phase diagrams for irreversibility in sheared adhesive suspensions. (a) Critical strain amplitudes due to collisions (left) or attractions (right). ω is normalized by $\tau_a \equiv 6\eta_0\epsilon^2a/A$. (b) Projection of the irreversibility map on the $(\phi, \omega\tau_a)$ plane. (c) Volume of the reversible absorbing states in the $(\phi, \omega\tau_a, \gamma_0)$ space.

states. This can be written as $\gamma_{0,\omega}^c = Sr_c A / 6\eta_0\epsilon^2a\omega$, which is independent of the volume fraction and thus must coexist with $\gamma_0^c(\phi)$ (hereafter $\gamma_{0,\phi}^c$). In between the two thresholds, *i.e.* $\gamma_{0,\omega}^c < \gamma_0 < \gamma_{0,\phi}^c$, suspensions can reach reversible absorbing states from any initial condition; below and above this range, irreversibility arises from either attractions (low γ_0) or collisions (high γ_0); see Fig. 5(a,b). However, $\gamma_{0,\omega}^c$ may also exceed $\gamma_{0,\phi}^c$, resulting in irreversible dynamics for all γ_0 . For example, consider a 40% suspension oscillating at 5 rad/s: if $\gamma_0 > 0.82$, the suspension is chaotic due to collisions [1, 2]; whereas if $\gamma_0 \leq 0.82$, it is irreversible due to attractions ($\gamma_{0,\omega}^c = 18.8$ for our suspensions). Note that, when $0.82 < \gamma_0 < 18.8$, both these mechanisms promote irreversibility. In such a case, the dynamics are controlled by collisions because collision-induced diffusions at larger γ_0 occur over a shorter time scale. We have checked that the suspension relaxation time (*i.e.* the time to reach steady states) is always orders-of-magnitude longer in our simulations and experiments (cf. Fig. 1) than those in Ref. [2]. Thus, for large values of γ_0 the system dynamics are collision-dominated: this finally explains why rate dependence is observed only for smaller γ_0 in OS, but not in SS, under the same shear rate.

A new phase diagram thus emerges for irreversibility in sheared adhesive suspensions. Fig. 5(b,c) shows the region of reversible steady dynamics in ϕ and ω , and the size of the reversibility window in γ_0 ; the latter is measured by a positive difference between the two critical amplitudes, $(\gamma_{0,\phi}^c - \gamma_{0,\omega}^c)^+$, where $(x)^+ = \max(x, 0)$.

Notice how rapidly the window reduces as ϕ or $1/\omega$ increases. Considering the chaotic nature of many-body systems (e.g. ideal gas, planets, etc.), microscopic irreversibility is rather the hallmark than an exception for suspensions. This is true even in Stokes flow for, whenever particles get close, their dynamics are not governed by the hydrodynamics alone. Here, by combining experiments with simulations, we have shown that there is a fundamental connection between irreversibility and suspension rheology, both of which depend on the strain amplitude as well as the driving frequency. Future work may examine this picture when including long-range hydrodynamic interactions, or explore the so-called active fluids whose intriguing rheologies defy reversibility even without passive particles [41].

We thank R. Radhakrishnan, C. Ness, F. Peters, A. Los, J. Chun and A. Leshansky for helpful discussions. The work is supported by the Swedish Research Council (grant no. VR 2014–5001) and University of Campania ‘L. Vanvitelli’ under the programme “VALERE: VANviteLli pEr la RicErca” project: SEND.

* zhoge@mech.kth.se

† mario.minale@unicampania.it

- [1] D. J. Pine, J. P. Gollub, J. F. Brady, and A. M. Leshansky, *Nature* **438**, 1476 (2005).
- [2] L. Corté, P. M. Chaikin, J. P. Gollub, and D. J. Pine, *Nat. Phys.* **4**, 420 (2008).
- [3] L. Corté, S. J. Gerbode, W. Man, and D. J. Pine, *Phys. Rev. Lett.* **103**, 248301 (2009).
- [4] J. M. Bricker and J. E. Butler, *J. Rheol.* **50**, 711 (2006).
- [5] J. M. Bricker and J. E. Butler, *Journal of Rheology* **51**, 735 (2007).
- [6] E. J. Hinch, *J. Fluid Mech.* **686**, 1–4 (2011).
- [7] R. N. Chacko, R. Mari, S. M. Fielding, and M. E. Cates, *Journal of Fluid Mechanics* **847**, 700–734 (2018).
- [8] C. Carotenuto, M. C. Merola, and M. Minale, *AIP Conference Proceedings* **1599**, 258 (2014).
- [9] R. Martone, L. P. Paduano, C. Carotenuto, and M. Minale, *AIP Conference Proceedings* **1981**, 020185 (2018).
- [10] R. Martone, C. Carotenuto, and M. Minale, *J. Rheol.* **64**, 1075 (2020).
- [11] P. Pham, J. E. Butler, and B. Metzger, *Phys. Rev. Fluids* **1**, 022201 (2016).
- [12] G. I. Menon and S. Ramaswamy, *Phys. Rev. E* **79**, 061108 (2009).
- [13] G. Düring, D. Bartolo, and J. Kurchan, *Phys. Rev. E* **79**, 030101 (2009).
- [14] J. R. Royer and P. M. Chaikin, *Proceedings of the National Academy of Sciences* **112**, 49 (2015).
- [15] C. Ness and M. E. Cates, *Phys. Rev. Lett.* **124**, 088004 (2020).
- [16] D. Hexner and D. Levine, *Phys. Rev. Lett.* **114**, 110602 (2015).
- [17] S. Wilken, R. E. Guerra, D. J. Pine, and P. M. Chaikin, *Phys. Rev. Lett.* **125**, 148001 (2020).
- [18] C. Ness, R. Mari, and M. E. Cates, *Science Advances* **4**, 10.1126/sciadv.aar3296 (2018).
- [19] V. Breedveld, D. van den Ende, R. Jongschaap, and J. Mellema, *J. Chem. Phys.* **114**, 5923 (2001).
- [20] Y. Lin, N. Phan-Thien, and B. C. Khoo, *J. Rheol.* **57**, 1325 (2013).
- [21] G. Drazer, J. Koplik, B. Khusid, and A. Acrivos, *Journal of Fluid Mechanics* **460**, 307–335 (2002).
- [22] Z. Ge and L. Brandt, arXiv: 2005.12755 (2020).
- [23] J. F. Brady and G. Bossis, *Annual Review of Fluid Mechanics* **20**, 111 (1988).
- [24] R. Mari, R. Seto, J. F. Morris, and M. M. Denn, *J. Rheol.* **58**, 1693 (2014).
- [25] O. Cheal and C. Ness, *Journal of Rheology* **62**, 501 (2018).
- [26] All simulations consider bidisperse suspensions of 500 spheres, with size ratio 1.4, in a cubic box subject to Lees-Edwards boundary condition. In OS, only small amplitudes are used, $\gamma_0 = 0.05 \sim 0.2$, while frequency is controlled by adjusting the non-dimensional time scale.
- [27] L. Lobry, E. Lemaire, F. Blanc, S. Gallier, and F. Peters, *Journal of Fluid Mechanics* **860**, 682–710 (2019).
- [28] G. Chatté, J. Comtet, A. Niguès, L. Bocquet, A. Siria, G. Ducouret, F. Lequeux, N. Lenoir, G. Ovarlez, and A. Colin, *Soft Matter* **14**, 879 (2018).
- [29] E. Brown, N. A. Forman, C. S. Orellana, H. Zhang, B. W. Maynor, D. E. Betts, J. M. DeSimone, and H. M. Jaeger, *Nature Materials* **9**, 220 (2010).
- [30] A. Singh, S. Pednekar, J. Chun, M. M. Denn, and J. F. Morris, *Phys. Rev. Lett.* **122**, 098004 (2019).
- [31] Z. Ge, R. Martone, L. Brandt, and M. Minale, arXiv: 2006.04494 (2020).
- [32] J. Israelachvili, *Intermolecular and Surface Forces* (Academic Press, 2011).
- [33] J. Mewis and N. J. Wagner, *Colloidal suspension rheology* (Cambridge University Press, 2012).
- [34] The vertical discrepancy between simulations and experiments may be due to polydispersity of the glass beads or residual short-range repulsion forces that are not modeled numerically.
- [35] M. Doi, *Journal of Physics: Condensed Matter* **23**, 284118 (2011).
- [36] E. C. Eckstein, D. G. Bailey, and A. H. Shapiro, *J. Fluid Mech.* **79**, 191 (1977).
- [37] D. Leighton and A. Acrivos, *Journal of Fluid Mechanics* **177**, 109–131 (1987).
- [38] V. Breedveld, D. van den Ende, R. Jongschaap, and J. Mellema, *The Journal of Chemical Physics* **114**, 5923 (2001).
- [39] $\gamma_0^*(\phi)$ can be calculated from the power-law fit $C\phi^{-\alpha}$ reported in Ref. [1]. However, there is a typo for the value of α . It should be 1.93 instead of -1.93 .
- [40] In general, the onset of rate dependence may depend on ϕ through a critical suspension shear stress, $\sigma^* \sim \eta_R^*(\phi)Sr_c$, since rheological quantities average over the entire suspension. In our case, $\eta_R^*(\phi)$ differs at most by a factor of 4 at large Sr , thus we refrain from introducing a ϕ dependence in Sr_c for simplicity.
- [41] D. Saintillan, *Annual Review of Fluid Mechanics* **50**, 563 (2018), <https://doi.org/10.1146/annurev-fluid-010816-060049>.